

# Robust Attributed Graph Alignment via Joint Structure Learning and Optimal Transport

Jianheng Tang<sup>2</sup>, Weiqi Zhang<sup>2</sup>, Jiajin Li<sup>3</sup>, Kangfei Zhao<sup>4</sup>, Fugee Tsung<sup>1,2</sup>, Jia Li<sup>1,2\*</sup>

<sup>1</sup>Hong Kong University of Science and Technology (Guangzhou),

<sup>2</sup>Hong Kong University of Science and Technology,

<sup>3</sup>Stanford University, <sup>4</sup>Tencent AI Lab

{jtangbf,wzhangcd}@connect.ust.hk, jiajinli@stanford.edu, zkf1105@gmail.com, {season,jialee}@ust.hk

**Abstract**—Graph alignment, which aims at identifying corresponding entities across multiple networks, has been widely applied in various domains. As the graphs to be aligned are usually constructed from different sources, the inconsistency issues of structures and features between two graphs are ubiquitous in real-world applications. Most existing methods follow the “embed-then-cross-compare” paradigm, which computes node embeddings in each graph and then processes node correspondences based on cross-graph embedding comparison. However, we find these methods are unstable and sub-optimal when structure or feature inconsistency appears. To this end, we propose SLOTAAlign, an unsupervised graph alignment framework that jointly performs Structure Learning and Optimal Transport Alignment. We convert graph alignment to an optimal transport problem between two intra-graph matrices without the requirement of cross-graph comparison. We further incorporate multi-view structure learning to enhance graph representation power and reduce the effect of structure and feature inconsistency inherited across graphs. Moreover, an alternating scheme based algorithm has been developed to address the joint optimization problem in SLOTAAlign, and the provable convergence result is also established. Finally, we conduct extensive experiments on six unsupervised graph alignment datasets and the DBP15K knowledge graph (KG) alignment benchmark dataset. The proposed SLOTAAlign shows superior performance and strongest robustness over seven unsupervised graph alignment methods and five specialized KG alignment methods.<sup>1</sup>

**Index Terms**—Graph alignment, Unsupervised learning, Structure learning, Optimal transport

## I. INTRODUCTION

Graph alignment refers to the problem of identifying the node correspondences (i.e., anchor links) across different graphs. With graph data becoming ubiquitous in the Web era, graph alignment establishes connections between multiple networks and integrates them into a world-view network for subsequent analysis and downstream applications. Thus, graph alignment provides a comprehensive perspective for structured data compared with mining each individual network. As a well-established problem, graph alignment has received much attention due to its vast applicable tasks, e.g., linking accounts in different social network platforms [25], [26], [40], matching entities across different knowledge graphs [34], [45], [63], [69], integrating protein-protein interactions of different species

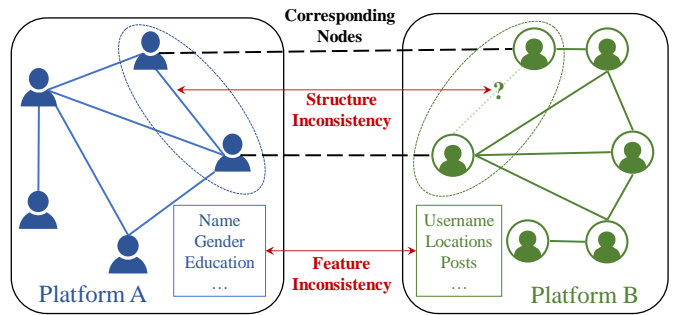


Fig. 1. An example of graph alignment with structure and feature inconsistency.

[21], [35], merging scholar profiles of academic collaboration networks [47], [67].

Graph alignment is usually treated as a supervised problem [33], [36], [67], [68], in which a set of ground-truth node correspondences is given. However, these correspondences are usually unavailable and further suffer from the labor expensiveness issue in real-world applications. Thus, unsupervised graph alignment methods have attracted increasing attention [4], [9], [14], [17], [19], [31], [72]. Also, graph nodes are often associated with wealthy side information, such as the user information of social network accounts or the embedding of knowledge graph entities. These high-dimensional node features/attributes can serve as an additional source of knowledge in graph alignment, especially under the unsupervised setting.

Most existing graph alignment methods rely on high-quality and well-measured graph structures. They require that the structure of the overlapped parts between two graphs is similar, which is named *structure consistency* thereafter. However, real-world graphs are often coupled with outliers [46] or with missing/irrelevant edges [28], [54], [61], leading to structure inconsistency across graphs. It is often observed that the same entities in different networks have quite different neighbors due to the structural noise [4], [72]. Figure 1 demonstrates an example of graph alignment on two social network platforms. Black dashed lines are anchor links that connect the same copies of users across two networks. As can be seen, two circled nodes are connected on Platform A, but their corresponding nodes on Platform B are not connected.

Besides structure inconsistency, another largely overlooked

\*Corresponding author.

<sup>1</sup>Code and data are released at <https://github.com/squareRoot3/SLOTAAlign>

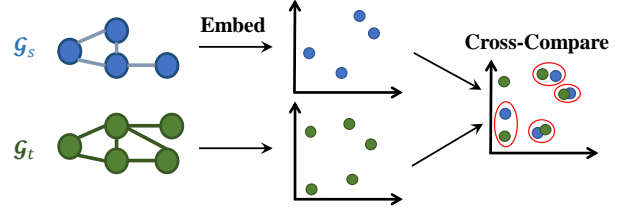
issue is that *node features in different graphs are usually unaligned and inconsistent*. Due to various functionalities of different networks (e.g., LinkedIn for job seeking and Twitter for opinion sharing), the same user in different networks commonly does not share the same features. Taking Figure 1 as an example, user information in Platform A includes the real name, gender, and education experiences, while Platform B contains the anonymized username, locations, posts, etc. Under this situation, corresponding nodes across two networks are not similar to each other and are incomparable. Likewise, in cross-lingual knowledge graph alignment, entities in different languages are usually embedded into individual feature spaces. Using machine translation [37], [44] can alleviate this issue, but may bring additional noise and cost.

In previous works, a popular paradigm for unsupervised graph alignment is the “embed-then-cross-compare” procedure [4], [9], [14], [17], [23], [31], as shown in Figure 2(a). As the name suggests, it first embeds nodes in each graph into a common feature space (e.g., using a graph neural network), and then compares embeddings across two graphs to obtain node correspondences. Nonetheless, we find this paradigm has the following limitations to deal with structure and feature inconsistency. First, as the node embeddings are calculated by aggregating information from the neighbors, it may amplify noise when structure inconsistency exists. Second, if features in two graphs are inconsistent, the corresponding node embeddings are also typically inconsistent and can not be compared directly [5], [14]. In knowledge graph alignment, margin-based ranking losses [44], [45] and contrastive learning [63] are frequently used to integrate embedding spaces across graphs. However, without the supervision of ground-truth node pairs, the process of embedding space integration is unstable and unreliable.

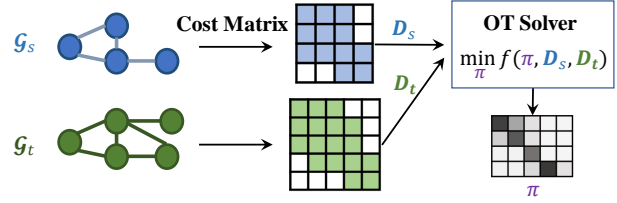
Besides the “embed-then-cross-compare” paradigm, another line of research is to reformulate the graph alignment problem as finding the optimal probabilistic correspondence between two probability measures on graphs. Specifically, Gromov-Wasserstein (GW) distance serves as an effective tool in modeling the correspondence problems between two graphs on unaligned metric spaces [30], [43]. We show the procedure of the resulting optimal transport based alignment in Figure 2(b). It first constructs two cost matrices  $D_s$  and  $D_t$  within each graph. Then, it applies an optimal transport solver to find the best transportation plan  $\pi$  with minimal cost according to  $D_s$  and  $D_t$ . The transportation plan  $\pi$  reveals node correspondences across graphs.

However, previous optimal transport based methods mainly consider the alignment between plain graphs without attributes and rely on manually designed cost matrices (e.g., the original graph adjacency matrix [30], [58], [60] or the heat kernel of graph Laplacian matrix [1], [6], [27]). Thus, these methods are potentially fragile to structure inconsistency. Moreover, how to find optimal cost matrices in attributed graphs for the optimal transport based alignment has not been well explored by existing methods. In summary, there is no satisfactory solution for enhancing the robustness of graph alignment

(a) The “Embed-Then-Cross-Compare” Alignment Paradigm



(b) Optimal Transport Based Alignment



(c) Joint Structure Learning and Optimal Transport Alignment

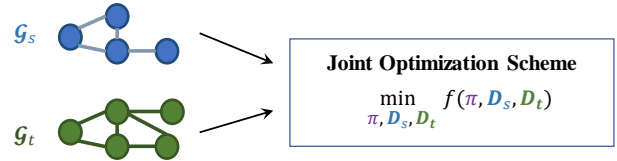


Fig. 2. Comparison between the existing graph alignment methods (top and middle) and our proposed SLOTAAlign framework (bottom).

against structure and feature inconsistency.

To address above issues, we propose a novel framework for joint Structure Learning and Optimal Transport Alignment (SLOTAAlign). As shown in Figure 2(c), SLOTAAlign simultaneously optimizes the intra-graph structure representation ( $D_s, D_t$ ) and cross-graph transportation plan  $\pi$  in a unified manner, which can get rid of choosing cost matrices manually. SLOTAAlign models the multi-view structure representation within each graph, which integrates the node-view, edge-view, and subgraph-view to reduce the effect of noise and inconsistency in original graph structures. Moreover, SLOTAAlign is more robust to feature inconsistency as it only utilizes intra-graph node relation and does not depend on cross-graph node embedding comparison. Additionally, we show that SLOTAAlign is invariant to graph feature permutation, which cannot be achieved by the “embed-then-cross-compare” methods. Theoretically, we provide an alternating scheme based algorithm to address the optimization problem arisen from SLOTAAlign, and establish the convergence result of the proposed algorithm.

To sum up, our contributions are three-fold:

- We point out and analyze that existing attributed graph alignment methods are susceptible to both structure and feature inconsistency, and thus perform unstably in noisy real-world graphs.
- A novel framework — SLOTAAlign has been proposed for joint structure learning and optimal transport alignment. We prove the robustness guarantee of SLOTAAlign against feature permutation and develop a convergent alternating

scheme based algorithm to solve the optimization problem in SLOTAAlign.

- We conduct extensive experiments on six graph alignment datasets and the DBP15K KG alignment benchmark dataset.

The proposed SLOTAAlign shows superior performance over seven general unsupervised graph alignment methods and five specialized KG alignment methods. It also has strongest robustness against multiple types of structure and feature inconsistency.

The rest of the paper is organized as follows. Section II introduces some preliminary knowledge about graph alignment and Gromov-Wasserstein distance. Section III analyzes the inconsistency issue for graph alignment. Section IV presents the proposed unsupervised graph alignment framework SLOTAAlign. Section V reports the experimental results. Related works and conclusion are presented in Section VI and Section VII respectively.

## II. PRELIMINARY

We denote an undirected attributed graph as  $\mathcal{G} = \{\mathcal{V}, \mathbf{A}, \mathbf{X}\}$ , where  $\mathcal{V} = \{v_1, v_2, \dots, v_n\}$  is the set of  $n$  nodes,  $\mathbf{A}$  is the adjacency matrix of the graph.  $A_{ij}$  equals to 1 if there is an unweighted edge between  $v_i$  and  $v_j$ , otherwise 0.  $\mathbf{X} \in \mathbb{R}^{n \times d}$  is the node feature matrix.  $\mathbf{x}_i = \mathbf{X}(i, :) \in \mathbb{R}^d$  is the feature vector of node  $v_i$ .

### A. Problem Statement

In this paper, we consider the problem of aligning two attributed graphs in an unsupervised manner. We refer to one graph as the source graph and the other as the target graph, denoted with  $\mathcal{G}_s$  and  $\mathcal{G}_t$  respectively. For each node in the source graph, graph alignment aims to identify, if any, the corresponding node in the target graph. Moreover, unsupervised alignment methods do not require any ground-truth node correspondences. We formulate this problem as follows.

**Definition 1** (Unsupervised Attributed Graph Alignment). *Given two attributed graphs  $\mathcal{G}_s = (\mathcal{U}_s, \mathbf{A}_s, \mathbf{X}_s)$  and  $\mathcal{G}_t = (\mathcal{V}_t, \mathbf{A}_t, \mathbf{X}_t)$ , without any observed node correspondences, the unsupervised graph alignment algorithm returns a set of aligned node pairs  $\mathcal{M} = \{(u_i, v_j) | (u_i, v_j) \in \mathcal{U}_s \times \mathcal{V}_t\}$ , where  $u_i$  and  $v_j$  are corresponding nodes across two graphs.*

### B. Gromov-Wasserstein Distance for Alignment

Conventional optimal transport needs a ground cost  $C$  to compare probability measures  $(\mu, \nu)$  and thus cannot be used if the measures are not defined on the same underlying space [41]. To address this limitation, the Gromov-Wasserstein (GW) distance was originally proposed in [39] for quantifying the distance between two probability measures supported on unaligned metric spaces. More precisely:

**Definition 2** (GW Distance). *Suppose that we are given two unregistered compact metric spaces  $(\mathcal{X}, d_X)$ ,  $(\mathcal{Y}, d_Y)$*

*accompanied with Borel probability measures  $\mu, \nu$  respectively. The GW distance between  $\mu$  and  $\nu$  is defined as*

$$\inf_{\pi \in \Pi(\mu, \nu)} \iint |d_X(x, x') - d_Y(y, y')|^2 d\pi(x, y) d\pi(x', y'),$$

*where  $\Pi(\mu, \nu)$  is the set of all probability measures on  $\mathcal{X} \times \mathcal{Y}$  with  $\mu$  and  $\nu$  as marginals.*

Intuitively, the GW distance is trying to preserve the isometric structure between two probability measures under the optimal derivation. If a map pairs  $x \rightarrow y$  and  $x' \rightarrow y'$ , then the distance between  $x$  and  $x'$  is supposed to be close to the distance between  $y$  and  $y'$ . Notably, the GW distance only requires modeling the topological or relational aspects of the distributions within each domain. In view of these nice properties, the GW distance has attracted intense research over the last decade, especially for structured data analysis, e.g., molecule analysis [48], [50], 3D shape matching [30], [43], graph embedding and classification [51], [53], generative models [3], [59], to name a few.

To apply the GW distance on the graph alignment problem, we consider the discrete case of Definition 2. Suppose  $\mu$  is a uniform distribution over all  $n$  nodes in the source graph  $\mathcal{G}_s$  and  $\nu$  is a uniform distribution over all  $m$  nodes in the target graph  $\mathcal{G}_t$ , i.e.,  $\mu = \frac{1}{n} \sum_{i=1}^n \delta_{u_i}$  and  $\nu = \frac{1}{m} \sum_{j=1}^m \delta_{v_j}$ , where  $\delta_{u_i}$  and  $\delta_{v_j}$  are one-hot signals on node  $u_i$  and  $v_j$ . The GW distance between  $\mu$  and  $\nu$  can be reformulated as:

$$\begin{aligned} \min_{\pi \in \Pi(\mu, \nu)} & \sum_{i=1}^n \sum_{j=1}^m \sum_{k=1}^m \sum_{l=1}^m |\mathbf{D}_s(i, j) - \mathbf{D}_t(k, l)|^2 \pi_{ik} \pi_{jl}, \\ \text{s.t. } & \pi \mathbf{1}_m = \mu, \pi^T \mathbf{1}_n = \nu, \pi \geq 0, \end{aligned} \quad (1)$$

where  $\mathbf{D}_s(i, j)$  can be considered as the transportation cost between  $u_i$  and  $u_j$  in  $\mathcal{G}_s$  (e.g., the edge  $\mathbf{A}_{ij}$ ), and  $\mathbf{D}_t(k, l)$  is the cost between  $v_k$  and  $v_l$  in  $\mathcal{G}_t$ . In (1), if  $\pi_{ik}$  and  $\pi_{jl}$  are large which indicates  $(u_i, v_k)$  and  $(u_j, v_l)$  are likely to be two node pairs, the difference of the corresponding intra-graph transportation costs should be similar, i.e.,  $|\mathbf{D}_s(i, j) - \mathbf{D}_t(k, l)| \rightarrow 0$ .

Accordingly, the GW distance optimization problem solves the optimal transport  $\pi$  merely based on two intra-graph cost matrices  $\mathbf{D}_s$  and  $\mathbf{D}_t$ . In graph alignment,  $\pi_{ik}$  indicates the matching score between  $u_i$  in  $\mathcal{G}_s$  and  $v_k$  in  $\mathcal{G}_t$ , and the alignment  $\mathcal{M}$  can be derived from  $\pi$ :

$$\mathcal{M} = \arg \max_{\mathcal{M} \in \mathbb{M}} \sum_{(u_i, v_k) \in \mathcal{M}} \pi_{ik}, \quad (2)$$

where  $\mathbb{M}$  is the set of all legit alignments.

## III. ANALYSIS OF THE INCONSISTENCY ISSUE

In this section, we discuss in-depth why structure inconsistency and feature inconsistency are challenging issues in the task of unsupervised graph alignment. As we mentioned before, a popular paradigm for solving graph alignment is first embedding nodes in two graphs as well as possible and second converting it to a cross-graph computation problem in the embedding space, i.e., an “embed-then-cross-compare” procedure. More specifically, it first calculates node embeddings

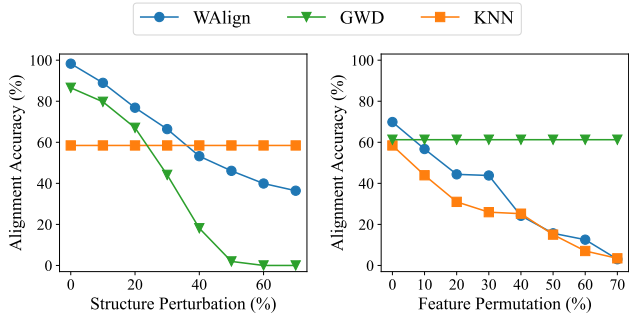


Fig. 3. Performance comparison of three graph alignment methods under different level of structure and feature inconsistency.

in each graph, for example, using a graph neural network. Then, it computes a set of node pairs  $\mathcal{M}$  based on the closeness of node embeddings across two graphs by solving the following embedding matching problem:

$$\min_{\mathcal{M} \in \mathbb{M}} \sum_{(u_i, v_j) \in \mathcal{M}} \|\mathbf{z}_{u_i} - \mathbf{z}_{v_j}\|, \quad (3)$$

where  $\mathbf{z}_{u_i}$  and  $\mathbf{z}_{v_j}$  denote the embeddings of node  $u_i$  in  $\mathcal{G}_s$  and node  $v_j$  in  $\mathcal{G}_t$ , respectively.

Nonetheless, this “embed-then-cross-compare” paradigm requires that  $\mathbf{z}_{u_i}$  and  $\mathbf{z}_{v_j}$  are in the same embedding space. When structures and features across two graphs are inconsistent, the corresponding node embeddings  $\mathbf{z}_{u_i}$  and  $\mathbf{z}_{v_j}$  are also typically unaligned and incomparable [5], [14]. Before matching node embeddings across graphs, we need to align the embedding spaces of two graphs, e.g., using a linear transformation  $\mathbf{Q}$ :

$$\min_{\mathcal{M} \in \mathbb{M}} \min_{\mathbf{Q}} \sum_{(u_i, v_j) \in \mathcal{M}} \|\mathbf{z}_{u_i} \mathbf{Q} - \mathbf{z}_{v_j}\|.$$

In the unsupervised graph alignment task, as none of the node correspondence is known,  $\mathbf{Q}$  is difficult to be calculated directly. On the other hand, because  $\mathbf{Q}$  is unknown, we are unable to compare node embeddings across graphs to obtain  $\mathcal{M}$ . To resolve this “chicken-and-egg” paradox, the adversarial learning framework is adopted [4], [14], [72] to generate pseudo node correspondences or auxiliary learning signals. However, these methods still require two embedding spaces to be partially aligned, otherwise the stability of iterations is not guaranteed.

On another front, optimal transport based methods that use Gromov-Wasserstein distance for graph alignment are more resilient to feature inconsistency as they mainly consider the intra-graph structural information. But as the price, they may be more fragile to the inconsistency in graph structures.

To better illustrate the robustness issue of existing methods under structure and feature inconsistency. We use the Cora citation network [42], [62] with the first 100 feature columns as the source graph  $\mathcal{G}_s$  and generate the target graph  $\mathcal{G}_t$  by producing different levels of inconsistency in  $\mathcal{G}_s$ . To control structure inconsistency, we randomly perturb  $p\%$  edges in  $\mathcal{G}_t$  to other previous unconnected positions and keep node features unchanged. For feature inconsistency, we fix the edge perturbation ratio to 25% and randomly permute the order of  $p\%$  feature columns in  $\mathcal{G}_t$ .

We compare the alignment performance of **WAlign** [14], the start-of-the-art unsupervised graph alignment method based on adversarial training, with **GWD** [60], a GW distance based method using graph adjacency matrices as cost matrices for alignment, and K-Nearest Neighbor (**KNN**), a simple baseline that directly matches nodes according to feature similarity. In Figure 3, we observe that the performance of WAlign is significantly affected by both structure and feature inconsistency. For example, when structure perturbation ratio is larger than 40%, WAlign is beat by KNN. Likewise, when feature permutation ratio is greater than 40%, the performance of WAlign is also very close to KNN. As for GWD, it is not influenced by any degree of feature inconsistency, but is more vulnerable to structure inconsistency.

Due to the above robustness issues in previous methods, in this work, we approach the graph alignment task via intra-graph structure modeling and cross-graph optimal transport alignment in a unified manner. We take the advantages of both embedding-based methods and optimal transport based methods, and show that it is more robust against structure and feature inconsistency. We introduce the proposed approach in the next section.

#### IV. METHODOLOGY

We propose a unified framework, SLOTAAlign, that jointly performs Structure Learning and Optimal Transport Alignment. As introduced in section II, the Gromov-Wasserstein (GW) distance is able to establish a connection between two graphs on unaligned metric spaces. With the help of the GW distance, the graph alignment task can be regarded as an optimal transport problem between two intra-graph matrices without the requirement of cross-graph comparison. However, most existing optimal transport based methods only consider the alignment between plain graphs and rely on a fundamental assumption that original graph structure can be viewed as ground-truth information for alignment. Unfortunately, such assumption is usually violated in real-world scenarios as we discussed in Section I and III. Although the Fused GW Distance [48] attempts to take node attributes into consideration, the cost matrices are still manually constructed which are fragile to the structure and feature inconsistency in real-world graphs.

To navigate such a pitfall, we are motivated to learn an optimal representation of the graph structure for alignment. We design a multi-view structure representation, including the node-view, edge-view, and subgraph-view, to model different perspectives of the original graph. We then develop a joint structure learning and alignment framework, which finds the optimal structure representation and node correspondences simultaneously. Figure 4 illustrates the framework of SLOTAAlign.

##### A. Multi-view Structure Modeling

Based on Equation (1), the optimization objective of the GW distance can be rewritten by

$$F(\pi) = \frac{1}{n^2} \sum_{i=1}^n \sum_{j=1}^n \mathbf{D}_s(i, j)^2 + \frac{1}{m^2} \sum_{k=1}^m \sum_{l=1}^m \mathbf{D}_t(k, l)^2 - 2\text{tr}(\mathbf{D}_s \pi \mathbf{D}_t \pi^T). \quad (4)$$

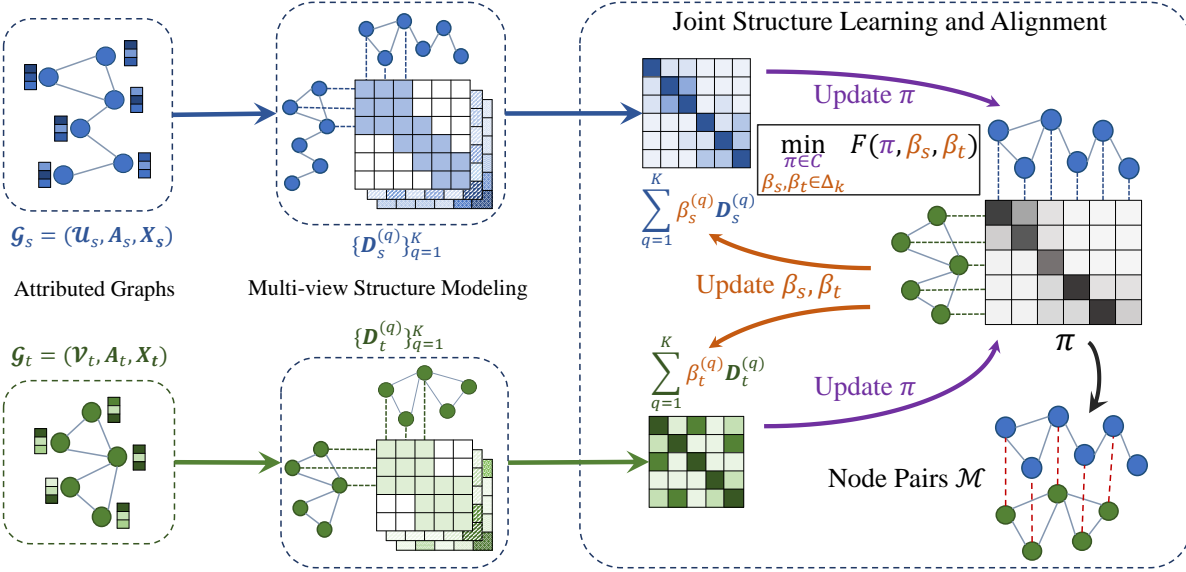


Fig. 4. The framework of SLOTAI. Given two attribute graphs, it first constructs a set of candidate structure views for each graph, and then optimizes the integrated structure representations and node correspondences simultaneously in the joint structure learning and graph alignment framework.

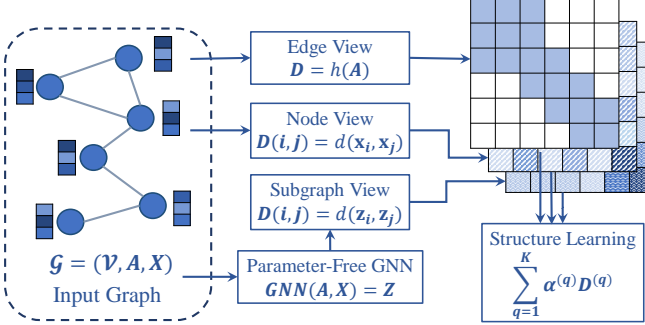


Fig. 5. The illustration of multi-view structure learning.

It is not hard to observe that the alignment quality from the GW distance heavily depends on how to construct two intra-graph cost matrices  $D_s$  and  $D_t$ . Instead of designing  $D_s$  and  $D_t$  manually, we first construct two sets of candidate graph structure bases  $\{D_s^{(q)}\}_{q=1}^K$  and  $\{D_t^{(q)}\}_{q=1}^K$  that enhance the original structure from multiple different views. As shown in Figure 5, we consider the following perspectives in multi-view structure modeling:

**(1) Edge-view.** It models the new graph structure as a function of the original adjacency matrix, i.e.,  $D = h(A)$ . Here  $h : \mathbb{R}^{n \times n} \rightarrow \mathbb{R}^{n \times n}$  can be any legit matrix mapping function such as the power up operator  $h(A) = A^k$ . For simplicity and efficiency in practice, we use the identity mapping:  $D = h(A) = A$ .

**(2) Node-view.** It uses pairwise node feature similarity to represent the new graph structure, i.e.,  $D(i, j) = d(\mathbf{x}_i, \mathbf{x}_j)$  where  $\mathbf{x}_i$  and  $\mathbf{x}_j$  are the feature vectors of node  $v_i$  and  $v_j$ , and  $d$  can be any similarity metric such as cosine similarity. Here we use the inner product to measure node similarity:  $D(i, j) = d(\mathbf{x}_i, \mathbf{x}_j) = \mathbf{x}_i^T \mathbf{x}_j$ , which is equivalent to cosine similarity after nodewise feature normalization.

Both the node-view and the edge-view consider the first-order relation between nodes. To model high-order interaction on the graph, we further construct the subgraph-view:

**(3) Subgraph-view.** It first integrates node features and neighbor information in the original structure using a Graph Neural Network (GNN), and then calculates the pairwise similarity between node embeddings. However, the training process of GNN may not be stable in unsupervised graph alignment, as discussed in Section III. Thus, we adopt a parameter-free GNN derived from the simplified graph convolutional network [57]. Specifically, we remove the parameterized linear layer and the activation function:

$$\mathbf{Z}^{(k)} = \hat{\mathbf{A}}^k \mathbf{X} = (\mathbf{M}^{-\frac{1}{2}} (\mathbf{A} + \mathbf{I}) \mathbf{M}^{-\frac{1}{2}})^k \mathbf{X} \quad (5)$$

where  $\mathbf{I}$  is the identity matrix,  $\mathbf{M}$  is the degree matrix of  $\mathbf{A} + \mathbf{I}$ , and  $\hat{\mathbf{A}} = \mathbf{M}^{-\frac{1}{2}} (\mathbf{A} + \mathbf{I}) \mathbf{M}^{-\frac{1}{2}}$  is the symmetric normalized adjacency matrix after adding self-loops for all nodes. After feature propagation for  $k$  steps, the node embedding  $\mathbf{Z}^{(k)}$  contains the  $k$ -hop neighborhood subgraph information of each node. Suppose  $\mathbf{z}_i^{(k)}$  is the embedding of node  $v_i$ , we also use the inner product to measure the  $k$ -order sub-graph similarity between nodes  $v_i$  and  $v_j$ :  $D(i, j) = d(\mathbf{z}_i^{(k)}, \mathbf{z}_j^{(k)}) = \mathbf{z}_i^{(k)T} \mathbf{z}_j^{(k)}$ ,  $k = 1, 2, 3, \dots$ .

To sum up, suppose  $K \geq 3$  is the maximum number of candidate structure bases, SLOTAI construct the following bases  $\{D_s^{(q)}\}_{q=1}^K$  for  $\mathcal{G}_s$ :

$$\begin{aligned} D_s^{(1)} &= \mathbf{A}_s \text{ (edge-view)}, & D_s^{(2)} &= \mathbf{X}_s \mathbf{X}_s^T \text{ (node-view)}, \\ D_s^{(q)} &= \hat{\mathbf{A}}_s^{q-2} \mathbf{X}_s (\hat{\mathbf{A}}_s^{q-2} \mathbf{X}_s)^T, 2 < q \leq K \text{ (subgraph-view)}. \end{aligned} \quad (6)$$

For  $\mathcal{G}_t$ , the construction process of  $\{D_t^{(q)}\}_{q=1}^K$  is the same.

#### B. Joint Structure Learning and Optimal Transport Alignment

After we construct multi-view graph structure bases  $\{D_s^{(q)}\}_{q=1}^K$  and  $\{D_t^{(q)}\}_{q=1}^K$ , a natural question is how to inte-

grate these candidate bases and learn an optimal representation of the graph structure. To this end, we model the new graph structure  $\mathbf{D}_s$  and  $\mathbf{D}_t$  as a convex hull of candidate structure bases. Specifically, we define

$$\mathbf{D}_s = \sum_{q=1}^K \beta_s^{(q)} \mathbf{D}_s^{(q)}, \quad \mathbf{D}_t = \sum_{q=1}^K \beta_t^{(q)} \mathbf{D}_t^{(q)}, \quad (7)$$

where  $\beta_s, \beta_t \in \Delta_K$ , i.e.,  $\sum_{q=1}^K \beta_s^{(q)} = 1, \beta_s^{(q)} \geq 0, \forall q \in [K]$ .

Subsequently, we target to optimize the weight vectors  $\beta_s, \beta_t$  and the transportation policy  $\pi$  in a unified Gromov-Wasserstein framework. More specifically, Equation (4) can be recast into the resulting optimization problem, i.e.,

$$\min_{\pi \in C, \beta_s, \beta_t \in \Delta_K} F(\pi, \beta_s, \beta_t), \quad (8)$$

where  $C = \{\pi \geq 0 : \pi 1_m = \mu, \pi^T 1_n = \nu\}$  and  $F(\cdot, \cdot)$  is a bi-quadratic function, i.e.,

$$\begin{aligned} F(\pi, \beta_s, \beta_t) = & \frac{1}{n^2} \sum_{i=1}^n \sum_{j=1}^n \left( \sum_{q=1}^K \beta_s^{(q)} \mathbf{D}_s^{(q)}(i, j) \right)^2 \\ & + \frac{1}{m^2} \sum_{k=1}^m \sum_{l=1}^m \left( \sum_{q=1}^K \beta_t^{(q)} \mathbf{D}_t^{(q)}(k, l) \right)^2 \\ & - 2\text{tr} \left( \left( \sum_{q=1}^K \beta_s^{(q)} \mathbf{D}_s^{(q)} \right) \pi \left( \sum_{q=1}^K \beta_t^{(q)} \mathbf{D}_t^{(q)} \right) \pi^T \right). \end{aligned} \quad (9)$$

Instead of purely finding the optimal probabilistic correspondence relationship in the vanilla GW problem, the proposed SLOTAIg is trying to learn the optimal structure representation and matching relationship simultaneously. To better understand the proposed SLOTAIg, we can consider a simple case — the weight vectors are vertices of the simplex, e.g.,  $\beta_s = \beta_t = (1, 0, \dots, 0)$ . Then, (8) will reduce to the vanilla model studied in previous work [60]. As such, if we minimize the GW objective on both  $\beta_s, \beta_t$  and  $\pi$ , the optimal solution returned from (8) will be better than the original one.

Next, we shed light on the robustness of SLOTAIg against feature inconsistency by a specific case — feature permutation.

**Definition 3** (Permutation on graph features). *Let  $\mathbf{P} \in \{0, 1\}^{d \times d}$  be any permutation matrix of order  $d$ , the feature permutation  $\mathcal{P}$  on a graph  $\mathcal{G} = \{\mathcal{V}, \mathbf{A}, \mathbf{X}\}$  is defined as a mapping of the node feature indices, i.e.,  $\mathcal{P}(\mathcal{G}) = \{\mathcal{V}, \mathbf{A}, \mathbf{X}\mathbf{P}\}$ .*

Feature permutation is very common in real-world cases, which represents two graphs sharing the same feature types but in different orders. Notably, methods based on “embed-then-cross-compare” are unstable to feature permutation as the feature space in  $\mathcal{G}_t$  is changed and no more aligned with  $\mathcal{G}_s$ . In comparison, SLOTAIg would not be affected by feature permutation according to the following proposition.

**Proposition 4.** SLOTAIg is invariant to feature permutation  $\mathcal{P}$  on  $\mathcal{G}_s$  or  $\mathcal{G}_t$ , e.g.,  $\text{SLOTAIg}(\mathcal{G}_s, \mathcal{G}_t) = \text{SLOTAIg}(\mathcal{G}_s, \mathcal{P}(\mathcal{G}_t))$

---

### Algorithm 1: SLOTAIg

---

**Input:** 1. Source graph  $\mathcal{G}_s = (\mathcal{U}_s, \mathbf{A}_s, \mathbf{X}_s)$   
2. Target graph  $\mathcal{G}_t = (\mathcal{V}_t, \mathbf{A}_t, \mathbf{X}_t)$   
3. Maximum number of iterations  $k_{max}$   
4. Number of candidate structure bases  $K$   
5. Step size of structure learning  $\tau$   
6. Step size in the Sinkhorn algorithm  $\eta$   
**Output:** Set of node correspondence pairs  $\mathcal{M}$

- 1 Initialize  $\beta_s^{(q)} \leftarrow \frac{1}{K}, \beta_t^{(q)} \leftarrow \frac{1}{K} (1 \leq q \leq K)$ ;
- 2 Initialize  $\alpha^1 \leftarrow [\beta_s, \beta_t]$ ;
- 3 Initialize  $\pi_{ij}^1 \leftarrow \frac{1}{nm} (1 \leq i \leq n, 1 \leq j \leq m)$ ;
- 4 Construct candidate structure bases  $\{\mathbf{D}_s^{(q)}\}_{q=1}^K$  and  $\{\mathbf{D}_t^{(q)}\}_{q=1}^K$  according to Equation (6);
- 5 **for**  $k = 1 \dots k_{max}$  **do**
- 6     Update  $\alpha^{k+1} \leftarrow \alpha^k$  according to Equation (11);
- 7     Update  $\pi^{k+1} \leftarrow \pi^k$  according to Equation (12);
- 8     **if**  $|\alpha^{k+1} - \alpha^k| < \epsilon_1$  and  $|\pi^{k+1} - \pi^k| < \epsilon_2$  **then**
- 9         | Break;
- 10     **end**
- 11 **end**
- 12 Generate node pairs  $\mathcal{M}$  according to Equation (2);

---

Assume that the structure bases of the permuted graph  $\mathcal{P}(\mathcal{G}_t) = \{\mathcal{V}, \mathbf{A}_t, \mathbf{X}_t \mathbf{P}\}$  are  $\{\overline{\mathbf{D}}_t^{(q)}\}_{q=1}^K$ , we have

$$\begin{aligned} \overline{\mathbf{D}}_t^{(1)} &= \mathbf{D}_t^{(1)}, \quad \overline{\mathbf{D}}_t^{(2)} = \mathbf{X}_t \mathbf{P} \mathbf{P}^T \mathbf{X}_t^T = \mathbf{X}_t \mathbf{X}_t^T = \mathbf{D}_t^{(2)}, \\ \overline{\mathbf{D}}_t^{(q)} &= \hat{\mathbf{A}}_t^{q-2} \mathbf{X}_t \mathbf{P} \mathbf{P}^T \mathbf{X}_t^T (\hat{\mathbf{A}}_s^{q-2})^T = \mathbf{D}_t^{(q)}, \quad 2 < q \leq K. \end{aligned} \quad (10)$$

Therefore, we have  $\{\overline{\mathbf{D}}_t^{(q)}\}_{q=1}^K = \{\mathbf{D}_t^{(q)}\}_{q=1}^K$ . As  $\mathcal{P}(\mathcal{G}_t)$  and  $\mathcal{G}_t$  have the same structure bases, the optimization problem (9) in SLOTAIg is unchanged, and we complete the proof. The robustness of the proposed SLOTAIg against more types of inconsistency has been further demonstrated in the experiment section.

### C. Optimization Algorithm

In this subsection, we provide a theoretically sound optimization algorithm to tackle (8). To proceed, we detect the hidden structure of (8) at first and further take it into account into the algorithmic development. We can observe that (8) is a nonconvex bi-quadratic program with polytope constraints. The basic strategy here is to optimize the weight  $\beta_s, \beta_t$  and the matching matrix  $\pi$  in an alternating fashion. As  $\beta_s$  and  $\beta_t$  are regarded as one block in our algorithm design, for simplicity, we use  $\alpha = [\beta_s, \beta_t]$  to represent the concatenation of  $\beta_s$  and  $\beta_t$ , i.e.,  $F(\pi, \alpha) = F(\pi, \beta_s, \beta_t)$ . More specifically, we adopt the proximal alternating linearized minimization strategy [2] here. To start with, we focus on the  $\alpha$  update:

$$\begin{aligned} \alpha^{k+1} &= \arg \min_{\alpha \in \Theta} \left\{ \nabla_{\alpha} F(\pi^k, \alpha^k)^T \alpha + \frac{1}{2\tau} \|\alpha - \alpha^k\|^2 \right\} \\ &= \text{Proj}_{\Theta} (\alpha^k - \tau \nabla_{\alpha} F(\pi^k, \alpha^k)). \end{aligned} \quad (11)$$

Here,  $\Theta = \{\alpha : \sum_{q=1}^K \alpha_q = \sum_{q=K+1}^{2K} \alpha_q = 1, \alpha_q \geq 0, \forall q \in [2K]\}$ . Due to the separable structure over  $\beta_s$  and  $\beta_t$ , (11) can be reduced to two simplex projection problems, which can be solved efficiently [11].

The crux of our algorithm is the  $\pi$ -update. As the projection onto the Birkhoff polytope (i.e.,  $C$ ) is rather computationally demanding, we are motivated to apply the entropic regularization to handle the  $\pi$ -update. Instead of the Euclidean distance  $\|\cdot\|^2$ , we invoke the Kullback-Leibler divergence. As such, the  $\pi$ -update is identical to the entropic optimal transport problem, and thus we can invoke the Sinkhorn algorithm to tackle it efficiently [8].

$$\pi^{k+1} = \arg \min_{\pi \in C} \left\{ \nabla_{\pi} F(\pi^k, \alpha^{k+1})^T \pi + \frac{1}{\eta} \mathbf{KL}(\pi \| \pi^k) \right\}, \quad (12)$$

where  $\mathbf{KL}(\cdot \| \cdot)$  is the Kullback-Leibler divergence, i.e.,

$$\mathbf{KL}(\mathbf{P} \| \mathbf{K}) \stackrel{\text{def.}}{=} \sum_{i,j} \mathbf{P}_{i,j} \log \left( \frac{\mathbf{P}_{i,j}}{\mathbf{K}_{i,j}} \right) - \mathbf{P}_{i,j} + \mathbf{K}_{i,j}.$$

We illustrate the detailed initialization and iteration process of SLOTAAlign in Algorithm 1. Given two sets of intra-graph structure bases, SLOTAAlign solves the optimization problem (8) by updating  $\alpha$  and  $\pi$  alternatively via Equation (11) and (12).

A further natural question is whether the proposed algorithm will converge or not. We answer the question in the affirmative.

**Theorem 5.** Suppose that  $0 < \tau < \frac{1}{L_f^\alpha}$  and  $0 < \epsilon < \eta < \frac{1}{L_f^\pi}$ , where  $L_f^\pi$  and  $L_f^\alpha$  are the gradient Lipschitz continuous modulus of  $F(\pi, \alpha)$  respectively. Then, any limit point of the sequence  $\{(\pi^k, \alpha^k)\}_{k \geq 0}$  converges to a critical point of  $\bar{F}(\pi, \alpha)$ , i.e.,

$$\bar{F}(\pi, \alpha) = F(\pi, \alpha) + \mathbf{I}_C(\pi) + \mathbf{I}_\Theta(\alpha),$$

where  $\mathbf{I}_C(\cdot)$  is the so-called indicator function on the set  $C$ .

*Proof.* As both  $C$  and  $\Theta$  are bounded sets, then  $\{(\pi^k, \alpha^k)\}$  is a bounded sequence. Subsequently, we target at proving the sufficient decrease property. As  $F(\cdot, \cdot)$  is a bi-quadratic function and the sequence  $\{(\pi^k, \alpha^k)\}_{k \geq 0}$ ,  $F(\pi, \alpha)$  is gradient Lipschitz continuous with modulus  $L_f^\pi$  and  $L_f^\alpha$ . To proceed, we revisit the  $\alpha$ -update at first,

$$\alpha^{k+1} = \arg \min_{\alpha \in \Theta} \left\{ \nabla_{\alpha} F(\pi^k, \alpha^k)^T \alpha + \frac{1}{2\tau} \|\alpha - \alpha^k\|^2 \right\}.$$

Since  $\alpha^{k+1}$  is the optimal solution of a strongly convex problem, we have

$$\begin{aligned} \nabla_{\alpha} F(\pi^k, \alpha^k)^T \alpha^k + \mathbf{I}_\Theta(\alpha^k) &\geq \\ \nabla_{\alpha} F(\pi^k, \alpha^k)^T \alpha^{k+1} + \mathbf{I}_\Theta(\alpha^{k+1}) + \frac{1}{2\tau} \|\alpha^{k+1} - \alpha^k\|^2. & \end{aligned}$$

Based on the gradient Lipschitz continuous property, it is easy to obtain,

$$\begin{aligned} F(\pi^k, \alpha^k) + \mathbf{I}_\Theta(\alpha^k) - F(\pi^k, \alpha^{k+1}) - \mathbf{I}_\Theta(\alpha^{k+1}) \\ \geq \left( \frac{1}{2\tau} - \frac{L_f^\alpha}{2} \right) \|\alpha^{k+1} - \alpha^k\|^2. \end{aligned}$$

On another front, we recall the  $\pi$ -update:

$$\pi^{k+1} = \arg \min_{\pi \in C} \left\{ \nabla_{\pi} F(\pi^k, \alpha^{k+1})^T \pi + \frac{1}{\eta} \mathbf{KL}(\pi \| \pi^k) \right\}.$$

Notably,  $\mathbf{KL}(\pi \| \pi^k)$  is 1-strongly convex on the Birkhoff polytope constraint, i.e.,

$$\mathbf{KL}(\pi^{k+1} \| \pi^k) \geq \frac{1}{2} \|\pi^{k+1} - \pi^k\|_F^2.$$

Similarly, we have

$$\begin{aligned} F(\pi^k, \alpha^{k+1}) + \mathbf{I}_C(\pi^k) - F(\pi^{k+1}, \alpha^{k+1}) - \mathbf{I}_C(\pi^{k+1}) \\ \geq \left( \frac{1}{2\eta} - \frac{L_f^\pi}{2} \right) \|\pi^{k+1} - \pi^k\|_F^2. \end{aligned}$$

To sum up, we get the desired result,

$$\begin{aligned} \bar{F}(\pi^{k+1}, \alpha^{k+1}) - \bar{F}(\pi^k, \alpha^k) \\ \leq -\kappa_1 \left( \|\pi^{k+1} - \pi^k\|_F^2 + \|\alpha^{k+1} - \alpha^k\|^2 \right), \end{aligned} \quad (13)$$

where  $\kappa_1 = \min \left( \frac{L_f^\alpha}{2} - \frac{1}{2\tau}, \frac{L_f^\pi}{2} - \frac{1}{2\eta} \right) > 0$  if  $0 < \tau < \frac{1}{L_f^\alpha}$  and  $0 < \epsilon < \tau < \frac{1}{L_f^\pi}$ . Summing up (13) from  $k = 0$  to  $+\infty$ , we obtain

$$\begin{aligned} \bar{F}(\pi^\infty, \alpha^\infty) - \bar{F}(\pi^0, \alpha^0) \\ \leq -\kappa_1 \sum_{k=0}^{\infty} \left( \|\pi^{k+1} - \pi^k\|_F^2 + \|\alpha^{k+1} - \alpha^k\|^2 \right). \end{aligned} \quad (14)$$

As the potential function  $\bar{F}(\cdot, \cdot)$  is bi-quadratic and thus coercive and  $\{(\pi^k, \alpha^k)\}_{k \geq 0}$  is a bounded sequence, it means the left-hand side is bounded, which implies

$$\begin{aligned} \sum_{k=0}^{\infty} \left( \|\pi^{k+1} - \pi^k\|_F^2 + \|\alpha^{k+1} - \alpha^k\|^2 \right) &< +\infty, \\ \alpha^{k+1} - \alpha^k \rightarrow 0, \pi^{k+1} - \pi^k \rightarrow 0. & \end{aligned}$$

Let  $(\pi^\infty, \alpha^\infty)$  be a limit point of the sequence  $\{(\pi^k, \alpha^k)\}_{k \geq 0}$ . Then, there exists a sequence  $\{n_k\}_{k \geq 0}$  such that  $\{(\pi^{n_k}, \alpha^{n_k})\}_{k \geq 0}$  converges to  $(\pi^\infty, \alpha^\infty)$ . To proceed, we write down the optimality condition w.r.t (11) and (12),

$$0 \in \nabla_{\alpha} F(\pi^k, \alpha^k) + \frac{1}{\tau} (\alpha^{k+1} - \alpha^k) + \mathcal{N}_\Theta(\alpha^k), \quad (15)$$

$$0 \in \nabla_{\pi} F(\pi^k, \alpha^{k+1}) + \frac{1}{\eta} (\log(\pi^{k+1}) - \log(\pi^k)) + \mathcal{N}_C(\pi^{k+1}), \quad (16)$$

where  $\mathcal{N}_C(x)$  is the normal cone of  $C$  at the point  $x$ . Replacing  $k$  by  $n_k$  in (15) and (16), taking limits on both sides as  $k \rightarrow \infty$

$$\begin{aligned} 0 &\in \nabla_{\alpha} F(\pi^\infty, \alpha^\infty) + \mathcal{N}_\Theta(\alpha^\infty), \\ 0 &\in \nabla_{\pi} F(\pi^\infty, \alpha^\infty) + \mathcal{N}_C(\pi^\infty), \end{aligned}$$

we obtain the desired result.  $\square$

Intuitively, the result in Theorem 5 guarantees that the sequence  $\{(\pi^k, \alpha^k)\}$  generated by SLOTAAlign will converge to a critical point of the nonconvex optimization problem (8).

#### D. Complexity Analysis

Suppose  $\mathcal{G}_s$  has  $n_s$  nodes,  $l_s$  edges, and  $d_s$  node attributes while  $\mathcal{G}_t$  has  $n_t$  nodes,  $l_t$  edges, and  $d_t$  node attributes. We first consider the case of dense graphs. The complexity of candidate bases construction in (6) is  $O(n_s^2 d_s + n_t^2 d_t)$ . The cost of calculating  $F(\pi, \alpha)$  in (9) is  $O(n_s^2 n_t + n_s n_t^2)$ . The cost of  $\alpha$ -update in (11) and  $\pi$ -update in (12) is  $O(n_s^2 n_t + n_s n_t^2)$ . Therefore, the overall complexity is  $O(n_s^2 d_s + n_t^2 d_t + n_s^2 n_t + n_s n_t^2)$ , which is the same order as other optimal transport based alignment methods [6], [30], [48], [60].

If  $\mathcal{G}_s$  and  $\mathcal{G}_t$  are large-scale sparse graphs, i.e.,  $n_s^2 \gg l_s$ ,  $n_t^2 \gg l_t$ ,  $n_s \gg d_s$ , and  $n_t \gg d_t$ , SLOTAIg can take advantage of the sparsity and low-rank properties of candidate structure bases  $\{\mathbf{D}_s^{(q)}\}_{q=1}^K$  and  $\{\mathbf{D}_t^{(q)}\}_{q=1}^K$  in calculating (9) and updating  $\alpha$  and  $\pi$ . In this case, SLOTAIg can be optimized to quadratic time complexity  $O(n_s n_t (d_s + d_t) + n_s l_t + n_t l_s)$ .

In the experiments, SLOTAIg is able to align graphs with about 20,000 nodes efficiently (e.g., the DBP15K dataset). To further scale up SLOTAIg linearly, recent divide-and-conquer methods [15], [63] can be adopted. For example, LIME [63] develops a bi-directional iterative graph partition strategy based on METIS [20] to divide large-scale graph pairs into smaller subgraph pairs, and then applies alignment methods for each subgraph pair. It can preserve 80% links when partitioning two graphs with millions of nodes into 75 subgraph pairs. Besides, LargeEA [15] develops a mini-batch generation strategy to partition large graphs into smaller mini-batches for alignment. Therefore, SLOTAIg has great potential to be applied to graphs with millions of nodes. As the main target of this paper is to propose a more accurate and robust graph alignment method, we leave the scalability issue as our future work.

## V. EXPERIMENTS

In this section, we assess the effectiveness of the proposed SLOTAIg model. We aim to answer the following questions:

- (Q1) Is SLOTAIg more robust to feature and structure inconsistency compared with other alignment methods?
- (Q2) Does SLOTAIg outperform the state-of-the-art methods on noisy real-world graph alignment applications?
- (Q3) Does the joint structure learning and optimal transport framework in SLOTAIg really benefit the alignment performance?
- (Q4) How sensitive is SLOTAIg to different hyperparameters?

Our code and data are provided in the supplementary materials, and will be publicly available upon acceptance.

#### A. Experimental Setup

We first introduce the experimental settings, including datasets, baseline methods, evaluation metrics, and implementation details.

**Datasets.** In Table I, we list the statistics of all datasets used in the experiments. Four semi-synthetic datasets with different degrees of structure and feature inconsistency are used to evaluate the robustness of SLOTAIg and baselines. Besides,

three noisy real-world graph alignment datasets are used to assess the overall performance of all methods. The four semi-synthetic datasets are:

- **Cora** and **Citeseer** [42] are two citation networks in which nodes correspond to scientific publications and edges are citation links. Each publication node in the graph is described by a 0/1-valued word vector indicating the absence/presence of the corresponding word from the dictionary, i.e., the bag-of-words feature.
- **PPI** [73] is a Protein-Protein Interaction network where nodes are proteins and edges indicate the interaction between proteins. Motif gene sets and immunological signatures are node features.
- **Facebook** [24] is a social network where nodes represent Facebook accounts and edges reflect relations between accounts. Node features are extracted from user profiles.

For the above four datasets, we follow the experimental setup in [5], [17]. We treat the original graph data as the source graph  $\mathcal{G}_s = \{\mathcal{U}_s, \mathbf{A}_s, \mathbf{X}_s\}$ , and perform node permutation to generate the corresponding target graph  $\mathcal{G}_t = \{\mathcal{V}_t, \mathbf{A}_t, \mathbf{X}_t\}$  for alignment. Specifically, we have  $\mathbf{A}_t = \mathbf{P}^T \mathbf{A}_s \mathbf{P}$  and  $\mathbf{X}_t = \mathbf{P}^T \mathbf{X}_s$ . Then we generate different levels of structure and feature inconsistency in  $\mathcal{G}_s$ . We introduce the detailed generation process in the next subsection.

Subsequently, we evaluate all methods on the following noisy real-world graph alignment datasets without further modification:

- **Douban Online-Offline.** In this scenario, we align two social network graphs, the online graph and the offline graph. In the online graph, nodes represent users, and edges represent the interaction between users (e.g., reply to a message) on the website. The offline graph is constructed according to the user's co-occurrence in social gatherings. The location of a user is used as node features in both graphs. The online graph is larger and contains all the users in the offline graph. In Douban, 1,118 users that appear in both graphs are used as the ground truth alignments.
- **ACM-DBLP.** In this scenario, we align two co-author networks ACM and DBLP, which are extracted from the publication information in four research areas. In both networks, nodes represent authors, and edges represent co-author relations. Node features indicate the number of papers that are published in different venues. There are 6,325 common authors across two networks used as the ground truth alignments.
- **DBP15K.** DBP15K [44] is a widely used KG alignment dataset. It consists of three cross-lingual entity alignment scenarios: DBP15K<sub>ZH\_EN</sub> (Chinese to English), DBP15K<sub>JA\_EN</sub> (Japanese to English), and DBP15K<sub>FR\_EN</sub> (French to English). All three subsets are created from multi-lingual DBpedia, and each contains 15,000 pairs of aligned entities. To preserve the feature inconsistency between multi-lingual knowledge graphs, we do not perform machine translation in data preprocessing. Instead, we follow [34] and use LaBSE [12], i.e., a multi-lingual BERT encoder, to extract 768-

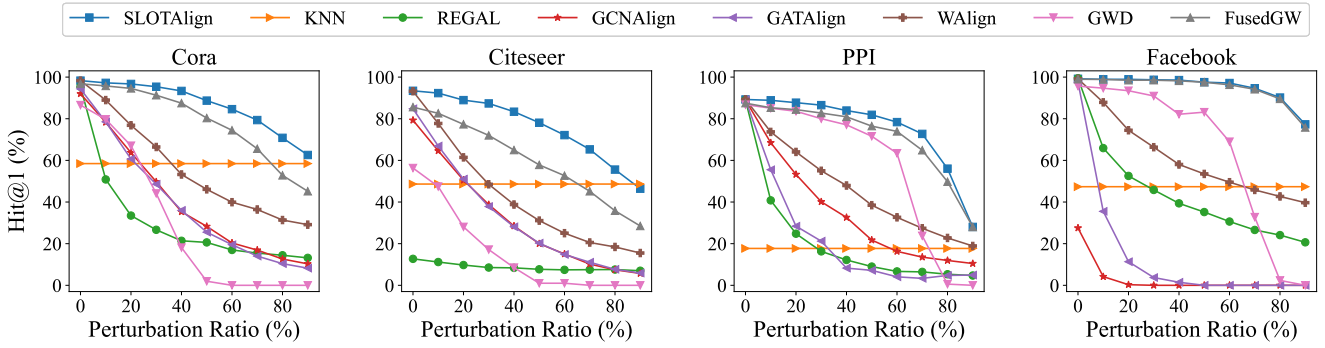


Fig. 6. Performance comparison of eight graph alignment methods under different levels of structure inconsistency.

TABLE I

DATA STATISTICS. ATTR. REPRESENTS THE NUMBER OF NODE ATTRIBUTES.

Dataset	# Nodes	# Edges	# Attr.	Description
Cora [42]	2,708	5,028	1,433	Citation Network
Citeseer [42]	3,327	4,732	3,703	Citation Network
PPI [73]	1,767	16,159	171	Protein Interaction
Facebook [24]	4,039	44,117	1,476	Social Network
Douban [65]	3,906	16,328	538	Social Network
-Online	1,118	3,022	538	Social Network
ACM-DBLP [66]	9,872	39,561	17	Co-Author Network
-DBLP	9,916	44,808	17	Co-Author Network
DBP15K <sub>ZH_EN</sub> [44]	19,388	70,414	768	Knowledge Graph
-EN	19,572	95,142	768	Knowledge Graph
DBP15K <sub>JA_EN</sub> [44]	19,814	77,214	768	Knowledge Graph
-EN	19,780	93,484	768	Knowledge Graph
DBP15K <sub>FR_EN</sub> [44]	19,661	105,998	768	Knowledge Graph
-EN	19,993	115,722	768	Knowledge Graph

dimensional node features from each entity name.

**Baselines.** We compare SLOTAlign with seven unsupervised graph alignment baselines, including KNN, four methods based on the “embed-then-cross-compare” paradigm (REGAL, WAlign, GCNAlign, and GATAAlign) and two optimal transport based methods (GWD and FusedGW). We introduce these baselines as follows:

- **KNN.** It is a simple baseline that directly matches nodes to top-k nearest neighbors in the feature space.
- **REGAL** [17]. It is a fast embedding-based graph alignment method that can be applied to graph with or without node features.
- **WAlign** [14]. It is a lightweight Graph Convolutional Network architecture with a Wasserstein distance discriminator to identify candidate node correspondences. These pseudo node correspondences are used to update network parameters and node embeddings.
- **GCNAlign** [56]. It uses the Graph Convolutional Network [22] to calculate node embeddings, and synthesizes pseudo node correspondence pairs based on the cross-graph embedding similarity. The network is trained by the margin-based ranking loss, which makes corresponding nodes closer in the embedding space.
- **GATAAlign** [52]. Its architecture is similar to GCNAlign mentioned above, but uses Graph Attention Network for

node embedding learning.

- **GWD** [60]. Similar to SLOTAlign, it invokes GW distance for graph alignment. However, it merely considers the structural information and uses the graph adjacency matrix to represent the cost matrices.
- **FusedGW** [48]. It extends the GW distance to a new framework that takes into account both structure and feature information on graphs for the attributed graph alignment problem.

**Evaluation Metrics.** We use **Hit@k** to evaluate the performance of all graph alignment methods. It calculates the percentage of the nodes in  $\mathcal{V}_t$  whose ground-truth alignment results in  $\mathcal{V}_s$  is in the top-k candidates. We use all node correspondences across two graphs in evaluation.

**Implementation Details.** For all mentioned baselines, we run the code provided by the authors and keep the default configuration. For SLOTAlign, we set the step size in the Sinkhorn algorithm  $\eta$  as 0.01 by default in all datasets. The step size of structure learning  $\tau$  is 0.1 in semi-synthetic datasets and 1 in real-world datasets. The number of candidate structure bases  $K$  is 2 in semi-synthetic datasets and 4 in real-world datasets. Our model is implemented based on PyTorch and DGL [55]. All experiments are performed on a high-performance computing server running Ubuntu 20.04 with an AMD Ryzen9 5950X CPU and an NVIDIA GeForce RTX 3090 GPU.

### B. (Q1) Alignment over Inconsistent Structures and Features

We first evaluate the robustness of the proposed SLOTAlign on four semi-synthetic datasets (Cora, Citeseer, PPI, and Facebook) against different degrees of structure inconsistency. To control the inconsistency level, we randomly perturb  $\%p$  edges in  $\mathcal{G}_t$  to other previous unconnected positions. In this setting, we only use the first 100 feature columns in Cora, Citeseer, and Facebook so that the models cannot only rely on node features for alignment.

We show the results of all compared methods in Figure 6. When the perturbation ratio is 0%, SLOTAlign has comparable performance with other start-of-the-art graph alignment methods. When the structure perturbation ratio  $p\%$  gradually increases from 0% to 70%, the performance of SLOTAlign degrades more slowly than other algorithms and consistently achieves the best in most cases. Note the maximum structure

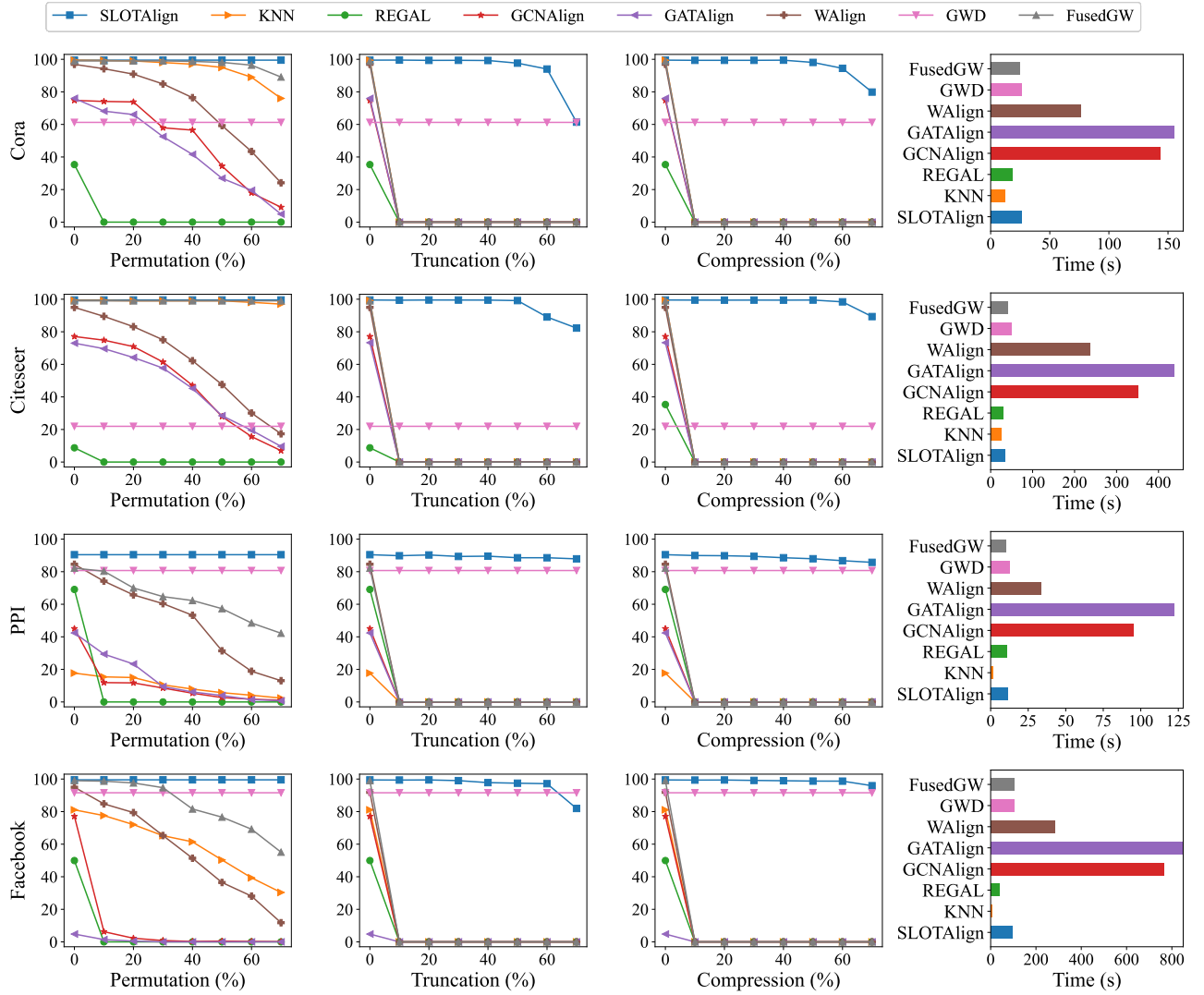


Fig. 7. Performance (Hit@1) and runtime comparisons of eight graph alignment methods under three types of feature inconsistency.

perturbation ratio in our setting is much larger compared with previous studies [5], [14], [17]. It validates that SLOTAlign is more resilient to structure inconsistency in graph alignment.

Subsequently, to evaluate the capability of each method in dealing with feature inconsistency, we consider three types of feature transformation on  $\mathcal{G}_t$ :

- **Feature Permutation.** We randomly permute  $p\%$  feature columns in  $\mathcal{G}_t$ , as defined in Definition 3.
- **Feature Truncation.** We randomly delete  $p\%$  feature columns in  $\mathcal{G}_t$ .
- **Feature Compression:** We use the Principal Component Analysis (PCA) to compress features in  $\mathcal{G}_t$  into a low-dimensional representation with compression ratio  $p\%$ .

These transformations can be regarded as three basic feature inconsistency simulators in real-world applications. For example, the Cora graph uses bag-of-words as node features to indicate the presence of a word in the document. First, consider that bag-of-words features in two graphs are built on the same vocabulary set but in different orders. This unaligned

scenario can be fully characterized by the feature perturbation simulator. Second, feature truncation simulates a scenario where the vocabulary used in  $\mathcal{G}_t$  is a subset of that in  $\mathcal{G}_s$ . Third, feature compression in this example can be interpreted as the alignment between sparse bag-of-words features in  $\mathcal{G}_s$  and dense low-dimensional features in  $\mathcal{G}_t$ .

For each transformation type, we gradually increase the inconsistency ratio  $p\%$  from 0% to 70%. We perturb 25% edges simultaneously to ensure that the models cannot align two graphs purely based on the structural information. We report the experimental results of SLOTAlign and other baselines in Figure 7 and analyze the model performance from the following perspectives.

**(1) Effect of Feature Permutation.** In the first column of Figure 7, we observe that the feature permutation has no influence on our proposed SLOTAlign, consistent with our proof in Proposition 4. In comparison, other methods using node features are significantly affected. For example, the Hit@1 of all baselines except GWD decreases to lower than 50% on

TABLE II  
EXPERIMENTAL RESULTS AND RUNTIME OF ALL COMPARED METHODS ON TWO REAL-WORLD GRAPH ALIGNMENT SCENARIOS.

Model	Douban Online-Offline					ACM-DBLP				
	Hit@1	Hit@5	Hit@10	Hit@30	Time(s)	Hit@1	Hit@5	Hit@10	Hit@30	Time(s)
KNN	3.31	10.38	16.64	30.05	0.9	49.25	59.46	63.42	69.61	4.5
REGAL	*30.32	*54.83	-	-	-	34.09	46.58	51.35	56.34	124.2
GCNAlign	20.93	34.44	39.62	50.72	248.3	38.43	68.46	77.64	86.89	5,821.3
GATAlign	23.70	36.94	44.01	57.16	264.5	14.21	34.07	42.12	49.00	7,298.2
WAlign	35.69	57.87	69.05	83.09	129.6	50.61	72.87	80.84	89.47	2,246.9
GWD	3.04	7.96	9.21	11.90	5.9	56.24	77.14	82.20	84.92	269.8
FusedGW	29.61	62.79	66.46	68.07	99.6	30.80	38.39	39.26	39.6	4,466.5
SLOTAlign	<b>51.43</b>	<b>73.43</b>	<b>77.73</b>	<b>82.02</b>	4.9	<b>66.04</b>	<b>84.06</b>	<b>87.95</b>	<b>90.32</b>	234.5
-w/o edge-view	2.42	10.02	16.37	32.11	4.1	30.42	48.16	53.26	58.59	224.6
-w/o node-view	36.23	56.17	60.82	65.65	4.1	0.35	1.19	1.85	4.16	228.9
-w/o subgraph-view	22.09	35.15	40.43	45.97	3.6	65.75	83.84	87.65	90.01	162.0
-fixed $\beta_s$ and $\beta_k$	3.67	12.61	18.96	31.22	4.8	26.56	46.43	54.42	64.16	187.9
-parameterized GNN	40.34	56.62	60.55	68.43	7.2	64.27	81.83	85.23	87.62	540.6

The results marked with \* are obtained from [14]. The rest of the results are reproduced by running the source code.

the PPI dataset when the permutation ratio increases to 70%. Although the structure-based approach GWD is not affected by any type and degree of feature inconsistency, its performance is also significantly lower than SLOTAlign as the feature information is not utilized.

**(2) Effect of Feature Truncation and Compression.** In the second and third columns of Figure 7, the performance of SLOTAlign keeps stable if the truncation or compression ratio is less than 50%. Even though the ratio is greater than 50%, SLOTAlign still outperforms the structure-based approach GWD, which verifies the robustness of SLOTAlign against different types and levels of feature inconsistency. On the contrary, other baselines using graph features fail to align two graphs with any level of feature truncation or compression. As we analyzed in Section III, these unsupervised methods are unable to perform cross-graph node embedding comparison if the embedding spaces of two graphs are not aligned.

**(3) Efficiency Comparison.** In the last column of Figure 7, we compare the computational efficiency of each method. REGAL has the shortest running time, but also the worst performance. SLOTAlign, GWD, and fusedGW have comparable running time as all of them are GW-based methods. Compared with graph neural network based methods WAlign, GCNAlign, and GCNAlign, SLOTAlign is more efficient on all datasets.

### C. (Q2) Alignment on Real-world Graphs

Next, we evaluate all methods on two noisy real-world graph alignment datasets, namely Douban Online-Offline and ACM-DBLP. The experimental results and runtime are reported in Table II. Our proposed SLOTAlign achieves the best performance in terms of the alignment accuracy on two datasets. Specifically, SLOTAlign has 15.7% and 15.4% absolutely improvement in Hit@1 on Douban and ACM-DBLP, respectively, compared with the state-of-the-art unsupervised alignment method WAlign. The performance improvement is also very significant compared with GW-based methods (GWD, FusedGW), proving the superiority of SLOTAlign. Besides,

TABLE III  
EVALUATION RESULTS OF ALL COMPARED KNOWLEDGE GRAPH ALIGNMENT METHODS ON DBP15K.

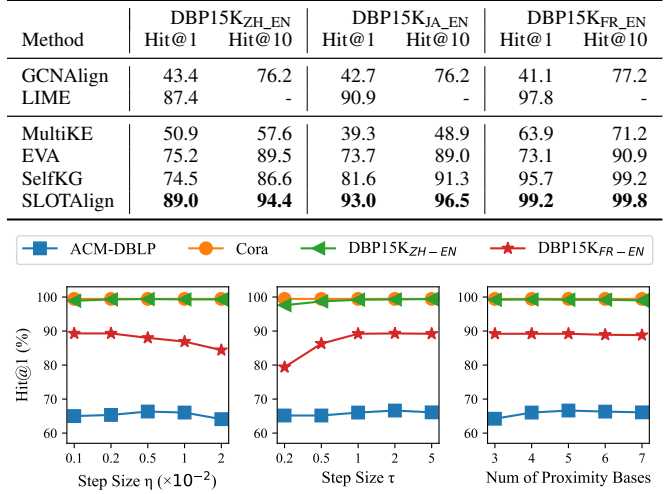


Fig. 8. Sensitivity analysis of SLOTAlign on four datasets.

SLOTAlign is time-efficient and only slower than two classic methods, KNN and REGAL.

We also evaluate SLOTAlign on the DBP15K dataset for KG alignment. To reduce the difficulty of large-scale optimization, we initialize  $\pi^1$  with the node-wise feature similarity matrix instead of the uniform distribution. We compare SLOTAlign with two supervised methods — GCNAlign [56] and LIME [63], and three unsupervised methods — MultiKE [64], EVA [32], and SelfKG [34]. The experimental results are summarized in Table III. Our proposed SLOTAlign achieves best performance on all the metrics. It corroborates our theoretical insights that SLOTAlign can better deal with the feature inconsistency issue in multi-lingual KG alignment. Since SLOTAlign focuses on the general attributed graph alignment problem, we do not consider the additional information in KG (e.g., relation type, entity description, and machine translation), even though they may further boost the performance [10], [29].

#### D. (Q3, Q4) Analysis of SLOTAlign

**Ablation Study.** To validate the effectiveness of each component in SLOTAlign, we compare it with several ablations. After removing each of the three views in the multi-view modeling, we obtain SLOTAlign without (w/o) edge-view, node-view, and subgraph-view. Besides, we conduct the ablation that does not perform structure learning, i.e., keep the weights of candidate structure bases  $\beta_s$  and  $\beta_t$  fixed in the optimization process. As shown in the bottom block of Table II, SLOTAlign consistently achieves the best performance compared with these variants, which validates the effectiveness of the proposed multi-view structure modeling and joint learning framework. In the last row of Table II, we compare the parameter-free GNN in subgraph-view with the original parameterized GNN [57] with linear layers and the ReLU activation function. We use the same loss in Equation (9) for GNN training. Although the parameterized GNN may have better expressive power in embedding-based alignment methods [34], [45], we find that it has inferior performance compared to the parameter-free GNN in SLOTAlign.

**Sensitivity Analysis of SLOTAlign.** We investigate the sensitivity of SLOTAlign to hyperparameters in Algorithm 1. On four datasets including ACM-DBLP, Cora, DBP15K<sub>ZH-EN</sub>, and DBP15K<sub>FR-EN</sub>, we analyze the performance of SLOTAlign with different step sizes of structure learning  $\tau \in \{0.2, 0.5, 1, 2, 5\}$ , different step sizes in the Sinkhorn algorithm  $\eta \in \{0.001, 0.002, 0.005, 0.01, 0.02\}$ , and different number of structure bases  $K = \{3, 4, 5, 6, 7\}$ . As shown in Figure 8, the performance of SLOTAlign is typically robust to all these hyperparameters. Without hyperparameter tuning, the default configuration (i.e.,  $\eta = 0.01, \tau = 1, K = 4$ ) is sufficient to get competitive results on these datasets.

## VI. RELATED WORK

**Supervised graph alignment** algorithms use a set of known seed node pairs between graphs to infer node correspondences. COSNET [68] uses an energy-based model to describe both global and local consistency. In addition, many embedding-based methods have been proposed to learn node embeddings and then predict corresponding node pairs [33], [36], [70]. For example, CrossMNA [7] considers inter-vector and intra-vector to combine graph and node embeddings, respectively. [13] propose a two-stage neural architecture to learn node embeddings and match nodes between graphs. ATTENT [71] utilizes active learning to improve graph alignment with limited seed pairs. BRIGHT [62] uses anchor links between seed pairs as landmarks to construct a certain unified space for matching by random walk. NEXTALIGN [67] reveals the close connections between graph convolutional networks and consistency-based alignment methods, and strikes a balance between the alignment consistency and disparity. Most existing knowledge graph (KG) alignment methods [12], [15], [32], [34], [38], [44], [45], [49], [56], [63], [64] also follow the “embed-then-cross-compare” paradigm. For example, AttrE [49] proposes the attribute character embeddings which shifts the entity embeddings from two KGs into the same space

for similarity calculation. LIME [63] learns the unified entity representations using a reciprocal alignment inference strategy to model the bi-directional entity interactions across graphs

**Unsupervised graph alignment** methods predict node correspondences across graphs without the requirement of any labeled node pairs. It has attracted increasing attention as node pairs are usually unavailable in real-world scenarios [14]. To solve this problem, FINAL [65] proposes the consistency principle, i.e., if two pairs of nodes are similar, their alignments should be consistent. HashAlign [16] leverages locality sensitive hashing to help node matching based on the node similarity obtained from graph structure and node features. REGAL [17] jointly obtains node representations from multiple graphs by factorizing matrix and matches the most similar node embedding across graphs. CONE-Align [5] proposes a proximity-preserving node embedding method to make different graphs comparable. GRASP [18] considers the graph alignment problem as a mapping between functions on graphs, and the node embeddings are interpreted as the linear combinations of eigenvectors. Kyster et al. [23] develop an enhanced algorithm variant based on REGAL, CONE-Align and GRASP. Karakasis et al. [19] propose to learn the node embeddings and matches the nodes of two graphs simultaneously. Considering the big success in various graph mining tasks, graph neural networks are integrated in graph alignment algorithms to acquire better node representations [14], [31], and adversarial learning strategies are utilized to further improve model performance [4], [9]. Besides, many unsupervised methods have been proposed for KG alignment [34], [37]. For example, SelfKG [34] uses the graph attention network to aggregate entity embeddings of one-hot neighbors, and proposes a relative similarity metric between the entities of two KGs for self-supervised contrastive learning.

## VII. CONCLUSION

In this paper, we propose SLOTAlign, the first robust unsupervised method tailored to tackle the structure and feature inconsistency issues in graph alignment. Instead of following the embed-then-cross-compare paradigm, we approach the graph alignment task via intra-graph structure modeling and cross-graph optimal transport alignment in a unified manner. Then, we present a provably convergent alternating type algorithm to address the joint optimization problem. Extensive experiments demonstrate that SLOTAlign can outperform the state-of-the-art graph alignment and KG alignment methods by an up to 15% absolute improvement in Hit@1 with a shorter running time, and is also the most robust model against structure and feature inconsistency.

## ACKNOWLEDGEMENTS

The research of Li was supported by NSFC Grant No. 62206067, Tencent AI Lab Rhino-Bird Focused Research Program RBFR2022008 and Guangzhou-HKUST(GZ) Joint Funding Scheme. The research of Tsung was supported by the Hong Kong RGC General Research Funds 16216119 and Foshan HKUST Projects FSUST20-FYTRI03B.

## REFERENCES

[1] Amélie Barbe, Marc Sebban, Paulo Gonçalves, Pierre Borgnat, and Rémi Gribonval. Graph diffusion wasserstein distances. In *Joint European Conference on Machine Learning and Knowledge Discovery in Databases*, pages 577–592. Springer, 2020.

[2] Jérôme Bolte, Shoham Sabach, and Marc Teboulle. Proximal alternating linearized minimization for nonconvex and nonsmooth problems. *Mathematical Programming*, 146(1):459–494, 2014.

[3] Charlotte Bunne, David Alvarez-Melis, Andreas Krause, and Stefanie Jegelka. Learning generative models across incomparable spaces. In *International Conference on Machine Learning*, pages 851–861. PMLR, 2019.

[4] Chaoqi Chen, Weiping Xie, Tingyang Xu, Yu Rong, Wenbing Huang, Xinghao Ding, Yue Huang, and Junzhou Huang. Unsupervised adversarial graph alignment with graph embedding. *arXiv preprint arXiv:1907.00544*, 2019.

[5] Xiyuan Chen, Mark Heimann, Fatemeh Vahedian, and Danai Koutra. Cone-align: Consistent network alignment with proximity-preserving node embedding. In *Proceedings of the 29th ACM International Conference on Information & Knowledge Management*, pages 1985–1988, 2020.

[6] Samir Chowdhury and Tom Needham. Generalized spectral clustering via gromov-wasserstein learning. In *International Conference on Artificial Intelligence and Statistics*, pages 712–720. PMLR, 2021.

[7] Xiaokai Chu, Xinxin Fan, Di Yao, Zhihua Zhu, Jianhui Huang, and Jingping Bi. Cross-network embedding for multi-network alignment. In *The world wide web conference*, pages 273–284, 2019.

[8] Marco Cuturi. Sinkhorn distances: Lightspeed computation of optimal transport. *Advances in neural information processing systems*, 26, 2013.

[9] Tyler Derr, Hamid Karimi, Xiaorui Liu, Jiejun Xu, and Jiliang Tang. Deep adversarial network alignment. In *Proceedings of the 30th ACM International Conference on Information & Knowledge Management*, pages 352–361, 2021.

[10] Qijie Ding, Daokun Zhang, and Jie Yin. Conflict-aware pseudo labeling via optimal transport for entity alignment. *arXiv preprint arXiv:2209.01847*, 2022.

[11] John Duchi, Shai Shalev-Shwartz, Yoram Singer, and Tushar Chandra. Efficient projections onto the  $l_1$ -ball for learning in high dimensions. In *Proceedings of the 25th international conference on Machine learning*, pages 272–279, 2008.

[12] Fangxiaoyu Feng, Yinfei Yang, Daniel Cer, Naveen Arivazhagan, and Wei Wang. Language-agnostic bert sentence embedding. In *Proceedings of the 60th Annual Meeting of the Association for Computational Linguistics*, pages 878–891, 2022.

[13] Matthias Fey, Jan E Lenssen, Christopher Morris, Jonathan Masci, and Nils M Kriege. Deep graph matching consensus. In *International Conference on Learning Representations*, 2019.

[14] Ji Gao, Xiao Huang, and Jundong Li. Unsupervised graph alignment with wasserstein distance discriminator. In *Proceedings of the 27th ACM SIGKDD Conference on Knowledge Discovery & Data Mining*, pages 426–435, 2021.

[15] Congcong Ge, Xiaoze Liu, Lu Chen, Yunjun Gao, and Baihua Zheng. Largeea: aligning entities for large-scale knowledge graphs. *Proceedings of the VLDB Endowment*, 15(2):237–245, 2021.

[16] Mark Heimann, Wei Lee, Shengjie Pan, Kuan-Yu Chen, and Danai Koutra. Hashalign: Hash-based alignment of multiple graphs. In *Pacific-Asia Conference on Knowledge Discovery and Data Mining*, pages 726–739. Springer, 2018.

[17] Mark Heimann, Haoming Shen, Tara Safavi, and Danai Koutra. Regal: Representation learning-based graph alignment. In *Proceedings of the 27th ACM international conference on information and knowledge management*, pages 117–126, 2018.

[18] Judith Hermanns, Anton Tsitsulin, Marina Munkhoeva, Alex Bronstein, Davide Mottin, and Panagiotis Karras. Grasp: Graph alignment through spectral signatures. *arXiv preprint arXiv:2106.05729*, 2021.

[19] Paris A Karakasis, Aritra Konar, and Nicholas D Sidiropoulos. Joint graph embedding and alignment with spectral pivot. In *Proceedings of the 27th ACM SIGKDD Conference on Knowledge Discovery & Data Mining*, pages 851–859, 2021.

[20] George Karypis and Vipin Kumar. A fast and high quality multilevel scheme for partitioning irregular graphs. *SIAM Journal on scientific Computing*, 20(1):359–392, 1998.

[21] Ehsan Kazemi, Hamed Hassani, Matthias Grossglauser, and Hassan Pezeshgi Modarres. Proper: global protein interaction network alignment through percolation matching. *BMC bioinformatics*, 17(1):1–16, 2016.

[22] Thomas N. Kipf and Max Welling. Semi-supervised classification with graph convolutional networks. In *ICLR*, 2017.

[23] Alexander Frederiksen Kyster, Simon Daugaard Nielsen, Judith Hermanns, Davide Mottin, and Panagiotis Karras. Boosting graph alignment algorithms. In *Proceedings of the 30th ACM International Conference on Information & Knowledge Management*, pages 3166–3170, 2021.

[24] Jure Leskovec and Julian McAuley. Learning to discover social circles in ego networks. *Advances in neural information processing systems*, 25, 2012.

[25] Chaozhuo Li, Senzhang Wang, Hao Wang, Yanbo Liang, Philip S Yu, Zhoujun Li, and Wei Wang. Partially shared adversarial learning for semi-supervised multi-platform user identity linkage. In *Proceedings of the 28th ACM International Conference on Information and Knowledge Management*, pages 249–258, 2019.

[26] Chaozhuo Li, Senzhang Wang, Philip S Yu, Lei Zheng, Xiaoming Zhang, Zhoujun Li, and Yanbo Liang. Distribution distance minimization for unsupervised user identity linkage. In *Proceedings of the 27th ACM International Conference on Information and Knowledge Management*, pages 447–456, 2018.

[27] Jia Li, Jiajin Li, Yang Liu, Jianwei Yu, Yuetong Li, and Hong Cheng. Deconvolutional networks on graph data. *Advances in Neural Information Processing Systems*, 34:21019–21030, 2021.

[28] Jia Li, Mengzhou Liu, Honglei Zhang, Pengyun Wang, Yong Wen, Lujia Pan, and Hong Cheng. Mask-gvae: Blind denoising graphs via partition. In *Proceedings of the Web Conference 2021*, pages 3688–3698, 2021.

[29] Jia Li and Dandan Song. Uncertainty-aware pseudo label refinery for entity alignment. In *Proceedings of the ACM Web Conference 2022*, pages 829–837, 2022.

[30] Jiajin Li, Jianheng Tang, Lemin Kong, Huikang Liu, Jia Li, Anthony Man-Cho So, and Jose Blanchet. Fast and provably convergent algorithms for gromov-wasserstein in graph learning. *arXiv preprint arXiv:2205.08115*, 2022.

[31] Zhehan Liang, Yu Rong, Chenxin Li, Yunlong Zhang, Yue Huang, Tingyang Xu, Xinghao Ding, and Junzhou Huang. Unsupervised large-scale social network alignment via cross network embedding. In *Proceedings of the 30th ACM International Conference on Information & Knowledge Management*, pages 1008–1017, 2021.

[32] Fangyu Liu, Muhan Chen, Dan Roth, and Nigel Collier. Visual pivoting for (unsupervised) entity alignment. In *Proceedings of the AAAI Conference on Artificial Intelligence*, volume 35, pages 4257–4266, 2021.

[33] Li Liu, William K Cheung, Xin Li, and Lejian Liao. Aligning users across social networks using network embedding. In *Ijcai*, pages 1774–1780, 2016.

[34] Xiao Liu, Haoyun Hong, Xinghao Wang, Zeyi Chen, Evgeny Kharlamov, Yuxiao Dong, and Jie Tang. Selfkg: Self-supervised entity alignment in knowledge graphs. In *Proceedings of the ACM Web Conference 2022*, pages 860–870, 2022.

[35] Yangwei Liu, Hu Ding, Danyang Chen, and Jinhui Xu. Novel geometric approach for global alignment of ppi networks. In *Thirty-First AAAI Conference on Artificial Intelligence*, 2017.

[36] Tong Man, Huawei Shen, Shenghua Liu, Xiaolong Jin, and Xueqi Cheng. Predict anchor links across social networks via an embedding approach. In *Ijcai*, volume 16, pages 1823–1829, 2016.

[37] Xin Mao, Wenting Wang, Yuanbin Wu, and Man Lan. From alignment to assignment: Frustratingly simple unsupervised entity alignment. In *Proceedings of the 2021 Conference on Empirical Methods in Natural Language Processing*, 2021.

[38] Xin Mao, Wenting Wang, Huimin Xu, Yuanbin Wu, and Man Lan. Relational reflection entity alignment. In *Proceedings of the 29th ACM International Conference on Information & Knowledge Management*, pages 1095–1104, 2020.

[39] Facundo Mémoli. Gromov-wasserstein distances and the metric approach to object matching. *Foundations of computational mathematics*, 11(4):417–487, 2011.

[40] Xin Mu, Feida Zhu, Ee-Peng Lim, Jing Xiao, Jianzong Wang, and Zhi-Hua Zhou. User identity linkage by latent user space modelling. In *Proceedings of the 22nd ACM SIGKDD International Conference on Knowledge Discovery and Data Mining*, pages 1775–1784, 2016.

[41] Gabriel Peyré, Marco Cuturi, et al. Computational optimal transport: With applications to data science. *Foundations and Trends® in Machine Learning*, 11(5-6):355–607, 2019.

[42] Prithviraj Sen, Galileo Namata, Mustafa Bilgic, Lise Getoor, Brian Galligher, and Tina Eliassi-Rad. Collective classification in network data. *AI magazine*, 29(3):93–93, 2008.

[43] Justin Solomon, Gabriel Peyré, Vladimir G Kim, and Suvrit Sra. Entropic metric alignment for correspondence problems. *ACM Transactions on Graphics (TOG)*, 35(4):1–13, 2016.

[44] Zequn Sun, Wei Hu, and Chengkai Li. Cross-lingual entity alignment via joint attribute-preserving embedding. In *International Semantic Web Conference*, pages 628–644. Springer, 2017.

[45] Zequn Sun, Qingheng Zhang, Wei Hu, Chengming Wang, Muhan Chen, Farahnaz Akrami, and Chengkai Li. A benchmarking study of embedding-based entity alignment for knowledge graphs. *Proceedings of the VLDB Endowment*, 13(12), 2020.

[46] Jianheng Tang, Jiajin Li, Ziqi Gao, and Jia Li. Rethinking graph neural networks for anomaly detection. In *International Conference on Machine Learning*, 2022.

[47] Jie Tang, Jing Zhang, Limin Yao, Juanzi Li, Li Zhang, and Zhong Su. Arnetminer: extraction and mining of academic social networks. In *Proceedings of the 14th ACM SIGKDD international conference on Knowledge discovery and data mining*, pages 990–998, 2008.

[48] Vayer Titouan, Nicolas Courty, Romain Tavenard, and Rémi Flamary. Optimal transport for structured data with application on graphs. In *International Conference on Machine Learning*, pages 6275–6284. PMLR, 2019.

[49] Bayu Distiawan Trisedy, Jianzhong Qi, and Rui Zhang. Entity alignment between knowledge graphs using attribute embeddings. In *Proceedings of the AAAI Conference on Artificial Intelligence*, volume 33, pages 297–304, 2019.

[50] Titouan Vayer, Laetitia Chapel, Rémi Flamary, Romain Tavenard, and Nicolas Courty. Fused gromov-wasserstein distance for structured objects: theoretical foundations and mathematical properties. *arXiv preprint arXiv:1811.02834*, 2018.

[51] Titouan Vayer, Rémi Flamary, Romain Tavenard, Laetitia Chapel, and Nicolas Courty. Sliced gromov-wasserstein. In *NeurIPS 2019-Thirty-third Conference on Neural Information Processing Systems*, volume 32, 2019.

[52] Petar Veličković, Guillem Cucurull, Arantxa Casanova, Adriana Romero, Pietro Lio, and Yoshua Bengio. Graph attention networks. *arXiv:1710.10903*, 2017.

[53] Cédric Vincent-Cuaz, Titouan Vayer, Rémi Flamary, Marco Corneli, and Nicolas Courty. Online graph dictionary learning. *arXiv preprint arXiv:2102.06555*, 2021.

[54] Bo Wang, Armin Pourshafeie, Marinka Zitnik, Junjie Zhu, Carlos D Bustamante, Serafim Batzoglou, and Jure Leskovec. Network enhancement as a general method to denoise weighted biological networks. *Nature communications*, 9(1):1–8, 2018.

[55] Minjie Wang, Da Zheng, Zihao Ye, Quan Gan, Mufei Li, Xiang Song, Jinjing Zhou, Chao Ma, Lingfan Yu, Yu Gai, Tianjun Xiao, Tong He, George Karypis, Jinyang Li, and Zheng Zhang. Deep graph library: A graph-centric, highly-performant package for graph neural networks. *arXiv:1909.01315*, 2019.

[56] Zhichun Wang, Qingsong Lv, Xiaohan Lan, and Yu Zhang. Cross-lingual knowledge graph alignment via graph convolutional networks. In *Proceedings of the 2018 conference on empirical methods in natural language processing*, pages 349–357, 2018.

[57] Felix Wu, Amauri Souza, Tianyi Zhang, Christopher Fifty, Tao Yu, and Kilian Weinberger. Simplifying graph convolutional networks. In *ICML*, pages 6861–6871, 2019.

[58] Hongteng Xu, Dixin Luo, and Lawrence Carin. Scalable gromov-wasserstein learning for graph partitioning and matching. *Advances in neural information processing systems*, 32:3052–3062, 2019.

[59] Hongteng Xu, Dixin Luo, Lawrence Carin, and Hongyuan Zha. Learning graphons via structured gromov-wasserstein barycenters. In *Proceedings of the AAAI Conference on Artificial Intelligence*, volume 35, pages 10505–10513, 2021.

[60] Hongteng Xu, Dixin Luo, Hongyuan Zha, and Lawrence Carin Duke. Gromov-wasserstein learning for graph matching and node embedding. In *International conference on machine learning*, pages 6932–6941. PMLR, 2019.

[61] Jiarong Xu, Yang Yang, Chunping Wang, Zongtao Liu, Jing Zhang, Lei Chen, and Jiangang Lu. Robust network enhancement from flawed networks. *IEEE Transactions on Knowledge and Data Engineering*, 2020.

[62] Yuchen Yan, Si Zhang, and Hanghang Tong. Bright: A bridging algorithm for network alignment. In *Proceedings of the Web Conference 2021*, pages 3907–3917, 2021.

[63] Weixin Zeng, Xiang Zhao, Xinyi Li, Jiuyang Tang, and Wei Wang. On entity alignment at scale. *The VLDB Journal*, pages 1–25, 2022.

[64] Qingheng Zhang, Zequn Sun, Wei Hu, Muhan Chen, Lingbing Guo, and Yuzhong Qu. Multi-view knowledge graph embedding for entity alignment. In *IJCAI*, pages 5429–5435, 2019.

[65] Si Zhang and Hanghang Tong. Final: Fast attributed network alignment. In *Proceedings of the 22nd ACM SIGKDD International Conference on Knowledge Discovery and Data Mining*, pages 1345–1354, 2016.

[66] Si Zhang and Hanghang Tong. Attributed network alignment: Problem definitions and fast solutions. *IEEE Transactions on Knowledge and Data Engineering*, 31(9):1680–1692, 2018.

[67] Si Zhang, Hanghang Tong, Long Jin, Yinglong Xia, and Yunsong Guo. Balancing consistency and disparity in network alignment. In *Proceedings of the 27th ACM SIGKDD Conference on Knowledge Discovery & Data Mining*, pages 2212–2222, 2021.

[68] Yutao Zhang, Jie Tang, Zhilin Yang, Jian Pei, and Philip S Yu. Cosnet: Connecting heterogeneous social networks with local and global consistency. In *Proceedings of the 21th ACM SIGKDD international conference on knowledge discovery and data mining*, pages 1485–1494, 2015.

[69] Xiang Zhao, Weixin Zeng, Jiuyang Tang, Wei Wang, and Fabian Suchanek. An experimental study of state-of-the-art entity alignment approaches. *IEEE Transactions on Knowledge & Data Engineering*, (01):1–1, 2020.

[70] Fan Zhou, Lei Liu, Kunpeng Zhang, Goce Trajcevski, Jin Wu, and Ting Zhong. Deeplink: A deep learning approach for user identity linkage. In *IEEE INFOCOM 2018-IEEE Conference on Computer Communications*, pages 1313–1321. IEEE, 2018.

[71] Qinghai Zhou, Liangyue Li, Xintao Wu, Nan Cao, Lei Ying, and Hanghang Tong. Attent: Active attributed network alignment. In *Proceedings of the Web Conference 2021*, pages 3896–3906, 2021.

[72] Yang Zhou, Jiaxiang Ren, Ruoming Jin, Zijie Zhang, Jingyi Zheng, Zhe Jiang, Da Yan, and Dejing Dou. Unsupervised adversarial network alignment with reinforcement learning. *ACM Transactions on Knowledge Discovery from Data (TKDD)*, 16(3):1–29, 2021.

[73] Marinka Zitnik and Jure Leskovec. Predicting multicellular function through multi-layer tissue networks. *Bioinformatics*, 33(14):i190–i198, 2017.